

High Step-Up Full Bridge DC-DC Converter with Multi-Cell Diode-Capacitor Network

Yan Zhang^{1,2}, Xinying Li¹, Zheyu Miu¹, Kunal kundanam¹, Jinjun Liu¹, Yan-fei Liu²

¹State Key Lab of Electrical Insulation and Power Equipment, Xi'an Jiaotong University, Xi'an, Shaanxi, China

²Department of Electrical and Computer Engineering, Queen's University, Kingston, Canada

Email: zhangyanjtu@mail.xjtu.edu.cn

Abstract—The full bridge boost isolated DC-DC converter achieves high voltage gain by setting the turns ratio of high-frequency transformer. Compared with the transformer, diode-capacitor voltage boost cell is more suitable to achieve high voltage gain with both high efficiency and power density. However, multi-cell diode-capacitor network has inrush current issue and strict LC filter requirement which is not suitable to achieve high efficiency in relatively low switching frequency and large power application. In order to meet high step-up voltage regulation and compulsory electrical isolation due to public safety, this paper proposes a high step-up full bridge isolated DC-DC converter with multi-cell diode-capacitor network which exploits the features of multi-winding transformer and diode-capacitor voltage boost cell. It has the following advantages 1). increases voltage boost capability and avoid extreme large duty ratio. 2) achieves almost zero output voltage ripples which reducing the inductance in output LC filter, 3) reduces transformer turns ratio and magnetic component volume. Furthermore, it can use the transformer leakage inductor and resonant capacitor to achieve zero-current switching (ZCS), which is beneficial to increase efficiency.

Keywords—Diode-capacitor network; high voltage gain; full-bridge isolated DC-DC converter; multi-winding transformer; zero-current switching (ZCS)

I. INTRODUCTION

Given the efficiency and environmental benefits, solar and fuel cell generation systems have rapidly developed in recent years. In photovoltaic (PV) systems, it is difficult to realize a series connection of PV cells without incurring shadow effect [1]. Fuel cell and lightweight battery power supply system are promising in future hybrid electric vehicle, more-electric aircraft and vessel. However, the obvious characteristic of these dc sources is low voltage supply. The basic DC-DC converter has encountered voltage boost limitation due to the parasitic parameters of main circuit. Therefore, high step-up voltage boost capability is the requirement of power converter with low input voltage, high efficiency and high power density. It has been one of the key technical issues in aforementioned renewable energy generation .

Full-bridge isolated boost DC-DC converter shown in Fig.1 have been widely used in solar and fuel cell based medium and high power generation system due to some inherent advantages [2][3]. In order to increase output voltage, the secondary side is replaced with voltage doubler rectifier in Fig.2 [4]. However, the voltage boost ratio is still limited by setting the turns ratio

This work was supported in part by the State Key Laboratory of Electrical Insulation and Power Equipment under the Grant EIPE14112 and EIPE16310 and Power Electronics Science and Education Development Program of Delta Environmental & Educational Foundation.

of transformer. Compared with transformer, diode-capacitor voltage boost cell is more suitable to achieve high voltage gain with both high efficiency and high power density. With the increasing number of basic cells, voltage gain can be further increased. Moreover, it does not increase drive and control circuit complexity due to only one fully controllable switch.

Fig.3 shows two typical high step-up DC-DC converters with multi-cell diode-capacitor network [5]-[8]. Fig 3(a) is widely used in low power supply chips such as LT3482, and it operates with high switching frequency such as $f_s=1\text{MHz}$. However, in above renewable energy generation system, when f_s is not high enough, the directly energy charging and discharging between different capacitors causes large inrush current and increases switching loss significantly. For the circuit shown in Fig 3(b), besides the large inrush current, low pass filter is necessary due to pulsed DC voltage generated by diode-capacitor network. In high voltage gain application, the amplitude of pulsed DC voltage is large and output current is relatively small, thus, the large inductance L_f is required to limit the output current and voltage ripples [9].

In order to overcome the drawbacks of inrush current and strict LC filter requirement, this paper propose a high step-up full-bridge isolated DC-DC converter with multi-cell diode-capacitor network, which exploits the advantages of multi-windings transformer and diode-capacitor voltage boost cell. It

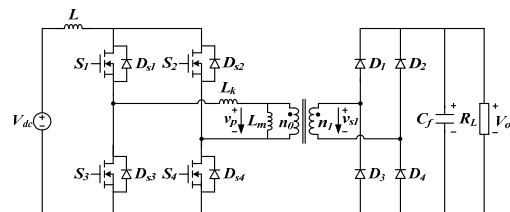


Fig.1 Full-bridge isolated boost DC-DC converter with diode rectifier.

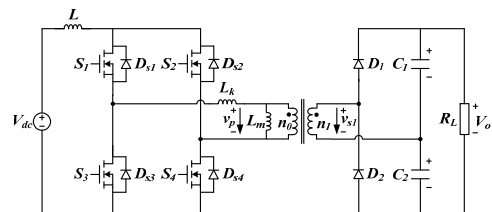
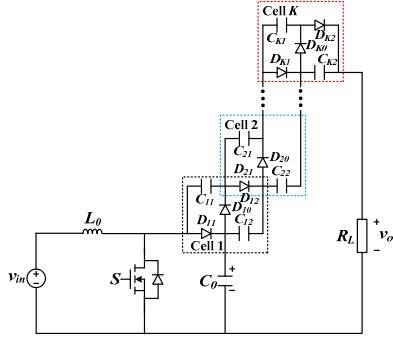
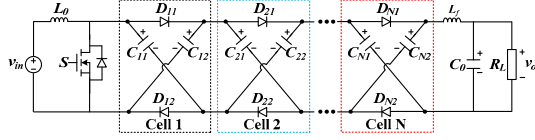


Fig.2 Full-bridge isolated boost DC-DC converter with voltage doubler rectifier.



(a) Series connection of multi-cell diode-capacitor network.



(b) Cascade connection of multi-cell diode-capacitor network.

Fig.3 High step-up DC-DC converters with multi-cell diode-capacitor network.

avoids the inrush current issue and achieves almost zero output voltage ripples. Meantime, it reduce transformer turns ratio and magnetic component volume which contributes to high power density. Section II describes the basic operation principle. Section III further provides control strategy and optimal parameters design to use the leakage inductor of transformer to realize zero-current switching (ZCS). Finally, simulation results are provided to verify the theoretical analysis.

II. OPERATION PRINCIPLE OF HIGH STEP-UP FULL BRIDGE ISOLATED DC-DC CONVERTER WITH MULTI-CELL DIODE-CAPACITOR NETWORK

Fig.4 shows one of the basic voltage boost cells: two-port diode-capacitor network. When D_{11} and D_{12} are conducting, C_{11} , C_{12} are connected in parallel and the terminal voltage meets:

$$v_2 = v_{C_{11}} = v_{C_{12}} = v_1 \quad (1)$$

When D_{11} and D_{12} are reversed blocked, C_{11} and C_{12} are connected in series and the terminal voltage meets:

$$v_2 = v_{C_{11}} + v_{C_{12}} - v_1 \quad (2)$$

Therefore, the LC filter is added in the output side to obtain the constant DC voltage.

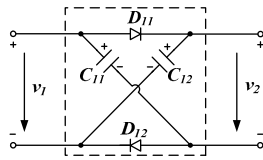


Fig.4 Basic diode-capacitor voltage boost cell.

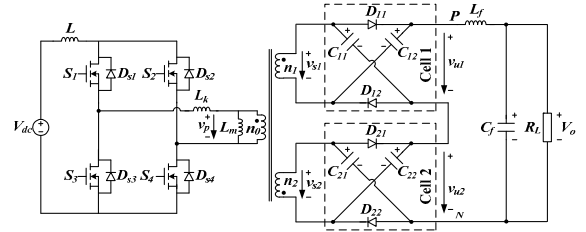


Fig.5 High step-up full-bridge isolated DC-DC converter with two-cell diode-capacitor network.

Fig.5 shows the proposed high step-up full-bridge isolated DC-DC converter with two-cell diode-capacitor network. The high-frequency transformer can be equivalent as an ideal transformer in parallel connection of magnetic inductor L_m and then in series connection of leakage inductor L_k . The first winding in the secondary side of transformer is connected to one two-port diode-capacitor cell in normal polarity and the second winding is connected to another two-port diode-capacitor cell in reversed polarity. The output of two diode-capacitor cells is connected in series to achieve high output voltage with essential LC filter.

For simple analysis, it is assumed that L_m is large enough ($L_k \ll L_m$) and i_{L_m} is continuous conduction. In the basic diode-capacitor boost cell, $C_{11} = C_{12}$ ($1 \leq i \leq N$). The detailed operation principles shown in Fig.6 are described as follows:

During $S_1 = S_2 = \text{ON}$, $S_3 = S_4 = \text{OFF}$ interval, DC source V_{dc} in series connection with boost inductor L charges the transformer primary side. The transformer magnetizing current is increasing linearly by ignoring the influence of leakage inductance L_k .

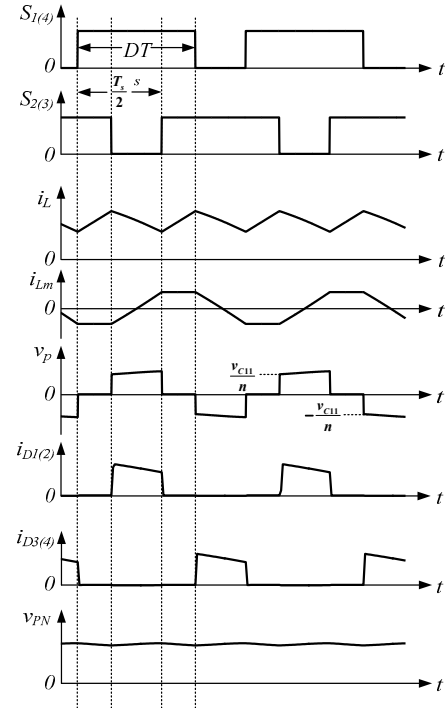


Fig.6 Operation principle of high step-up full bridge isolated DC-DC converter with two-cell diode-capacitor network.

$$L \frac{di_L}{dt} = V_{dc} - v_{p(S_1=S_4=ON)} \quad (3)$$

The transformer secondary side voltage v_{s1} , v_{s2} meet:

$$v_{s1(S_1=S_4=ON)} = \frac{n_1}{n_0} v_{p(S_1=S_4=ON)} \quad (4)$$

$$v_{s2(S_1=S_4=ON)} = -\frac{n_2}{n_0} v_{p(S_1=S_4=ON)} \quad (5)$$

Where: n_0 , n_1 , n_2 are the turns ratio of transformer primary and secondary side windings, respectively.

The induced voltage v_{s1} is positive, and D_{11} , D_{12} are conducting. n_1 winding charges two capacitor C_{11} and C_{12} in parallel connection.

$$v_{u1(S_1=S_4=ON)} = V_{C11} = v_{s1(S_1=S_4=ON)} \quad (6)$$

The inductive voltage v_{s2} is negative, and D_{21} , D_{22} are blocked. n_2 wind and two capacitors C_{21} , C_{22} are connected in series to supply the output side.

$$v_{u2(S_1=S_4=ON)} = -v_{s2} + 2V_{C21} \quad (7)$$

In this interval, the output voltage before filtered is

$$v_{PN(S_1=S_4=ON)} = v_{u1(S_1=S_4=ON)} + v_{u2(S_1=S_4=ON)} = 2V_{C21} + \frac{n_2}{n_1} V_{C11} + V_{C11} \quad (8)$$

During $S_1=S_2=S_3=ON$ interval, the transformer primary side winding n_0 is shorted and $v_p=0$. The DC source V_{dc} charges the boost inductor.

$$L \frac{di_L}{dt} = V_{dc} \quad (9)$$

In this interval, the induced transformer secondary side voltage $v_{s1}=v_{s2}=0$. All the diodes D_{11} , D_{12} , D_{21} and D_{22} in the transformer secondary side are blocked. The transformer secondary side winding n_1 and C_{11} , C_{12} , n_2 and C_{21} , C_{22} are connected in series to supply the output side. The output voltage before filtered is

$$v_{PN(S_1=S_2=S_3=ON)} = 2V_{C11} + 2V_{C21} \quad (10)$$

During $S_2=S_3=ON$, $S_1=S_4=OFF$ interval, DC source V_{dc} in series connection with boost inductor L charges the transformer primary side in reverse direction. The boost inductor current decreases linearly.

$$L \frac{di_L}{dt} = V_{dc} + v_{p(S_2=S_3=ON)} = V_{dc} - \frac{n_0}{n_2} V_{C21} \quad (11)$$

The induced transformer secondary side voltage v_{s1} is negative. D_{11} and D_{12} are blocked. n_1 winding and C_{11} , C_{12} are connected in series to supply the output side.

$$v_{u1(S_2=S_3=ON)} = v_{s1(S_2=S_3=ON)} + 2V_{C11} = \frac{n_1}{n_2} v_{s2(S_2=S_3=ON)} + 2V_{C11} \quad (12)$$

The induced transformer secondary side voltage v_{s2} is positive. D_{21} and D_{22} are conducting. n_2 winding charges two capacitors C_{21} , C_{22} in parallel connection. v_{s2} is clamped by v_{C21} .

$$v_{u2(S_2=S_3=ON)} = V_{C21} = -\frac{n_2}{n_0} v_{p(S_2=S_3=ON)} \quad (13)$$

The output voltage in this switching state is

$$v_{PN(S_2=S_3=ON)} = 2V_{C11} + \frac{n_1}{n_2} V_{C21} + V_{C21} \quad (14)$$

In steady state, the average voltage across the boost inductor L should be zero in one switching time period T_s . From (3), (9) and (11), we have

$$\left(V_{dc} - \frac{n_0}{n_1} V_{C11}\right)(1-D)T_s + \left(V_{dc} - \frac{n_0}{n_2} V_{C21}\right)(1-D)T_s + V_{dc}(2D-1)T_s = 0 \quad (15)$$

By solving the aforementioned equation, the voltage of the intermediate capacitor can be derived as

$$(1-D)\left(\frac{n_0}{n_1} V_{C11} + \frac{n_0}{n_2} V_{C21}\right) = V_{dc} \quad (16)$$

If two secondary side windings have the same turns ratio $n_1 : n_0 = n_2 : n_0 = n$, all the intermediate capacitors in the transformer secondary side have the same voltage, which can be calculated by solving (16).

$$V_C = \frac{n}{2} \cdot \frac{1}{1-D} V_{dc} \quad (17)$$

According to (8), (10) (14) and (17), v_{pn} has the same voltage and is almost constant.

$$v_{PN} = \frac{2n}{1-D} \cdot V_{dc} \quad (18)$$

Two diode-capacitor cells in the transformer secondary side operate in complementary mode to avoid inrush current and achieve zero output voltage ripples. Therefore, L_f is designed to eliminate the switching noisy and its value can be reduced to large extent.

In steady state, switches S_1 , S_4 or S_2 , S_3 have the same voltage stress, which is the maximum value of transformer primary side voltage v_p . The transformer secondary side voltage is clamped by intermediate capacitor when diodes are conducting. From (17), it can be derived as:

$$v_{S_Mos} = v_{p(S_1=S_4=ON, S_2=S_3=OFF)} = \frac{n_0}{n_1} V_{C11} = \frac{1}{2} \cdot \frac{1}{1-D} V_{dc} \quad (19)$$

All the diodes withstand the same voltage stress. The voltage across D_{11} and D_{12} during $S_2=S_3=ON$, $S_1=S_4=OFF$ interval is the reversed connection with v_{C11} and v_{s1} . It can be derived as:

$$v_{S_Diode} = v_{C11} - v_{s1(S_2=S_3=ON)} = \frac{n}{1-D} V_{dc} \quad (20)$$

With the increasing number of two-port diode-capacitor cells ($N=2k$), voltage gain of high step-up full bridge isolated DC-DC converter can be further increased. The main circuit is shown in Fig.7. Using the similar derivation approach, voltage gain, voltage stress of switch and diode can be rewritten as (21), (22) and (23).

$$G = \frac{v_o}{V_{dc}} = \frac{N \cdot n}{1-D} \quad (21)$$

$$v_{S_Mos} = \frac{1}{2} \frac{1}{1-D} V_{dc} = \frac{G}{2N \cdot n} V_{dc} \quad (22)$$

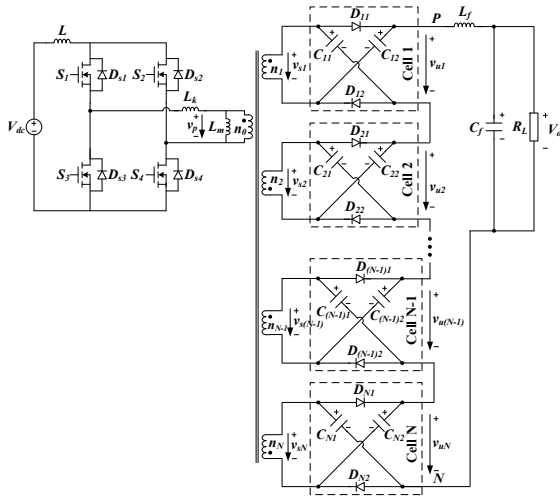


Fig.7 High step-up full-bridge isolated DC-DC converter with multi-cell diode-capacitor network.

$$v_{S_Diode} = \frac{n}{1-D} V_{dc} = \frac{G}{N} V_{dc} \quad (23)$$

Where: n is transformer primary, secondary winding turns ratio, N is the number of two-port diode-capacitor network, D is the duty ratio of switches.

Fig.8 shows the relationships of voltage gain and boost duty ratio D , transformer turns ratio n , and number of basic diode-capacitor cells N for high step-up full bridge isolated DC-DC converter with multi-cell diode-capacitor network. Fig.9 and 10 show the voltage stress of switching device and power diode, respectively. With the increasing number of basic diode-capacitor cell, the voltage stress of switch device and power diodes can be further reduced.

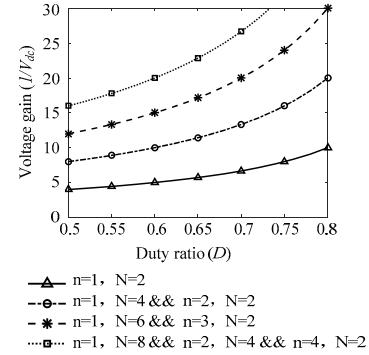


Fig.8 Voltage gain versus boost duty ratio.

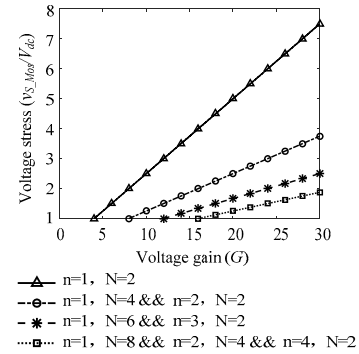


Fig.9 Voltage stress of switches.

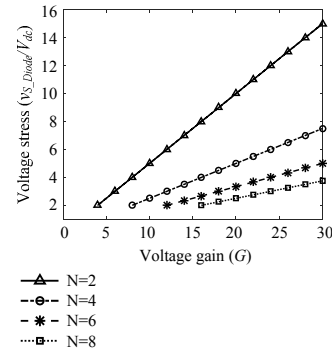


Fig.10 Voltage stress of power diodes.

III. ZERO CURRENT SWITCHING (ZCS) REALIZATION

The leakage inductor of transformer causes high voltage stress and spikes on the switching devices. In order to absorb the leakage energy and decrease switching loss, ZCS resonant circuit including L_k and C_r is provided. It suppresses voltage spikes of power switches and restrains the turn off di/dt of the secondary side diodes [4][10]. Fig.11 shows the ZCS resonant high-step full-bridge isolated DC-DC converter with two-cell diode-capacitor network ($N=2$). And Fig.12 shows the key waveforms of different interval in steady state. It includes 8 symmetrical operation modes in one switching time period T_s .

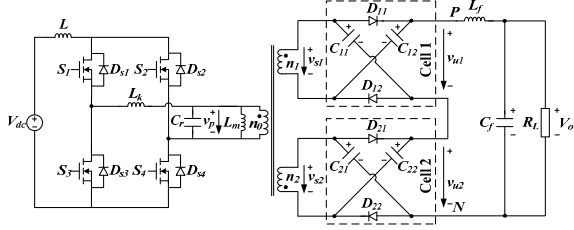


Fig.11 ZCS resonant high step-up full-bridge isolated DC-DC converter with two-cell diode-capacitor network.

Mode 1 (t_0-t_1): before t_0 instant, $S_1=S_4=OFF$, $S_2=S_3=ON$, diodes D_{21} and D_{22} are conducting. The resonant inductor current is the same as boost inductor current $i_{Lk}=-i_L$. At t_0 instant, S_1, S_4 are turned on, the drain source voltage v_{s1} and v_{s4} decrease to zero immediately. $S_1, S_2, S_3, S_4, D_{21}$ and D_{22} are conducting. L_k, C_r and L_m form resonant circuit. The voltage of capacitor C_r is clamped to v_{C21} . i_{Lk} is decreasing linearly by the rate of $v_{C21}/(nL_k)$. The current of switch S_1, S_4 increases and the current of S_2, S_3 decreases. During this interval, the state equations in time domain are:

$$v_{Cr}(t) = -\frac{1}{n}V_{C21} \quad (24)$$

$$i_{Lk}(t) = \frac{V_{C21}}{nL_k}(t-t_0) - i_L \quad (25)$$

$$i_{s1}(t) = i_{s4}(t) = \frac{1}{2}(i_L - (-i_{Lk}(t))) = \frac{1}{2} \frac{V_{C21}}{nL_k}(t-t_0) \quad (26)$$

$$i_{s2}(t) = i_{s3}(t) = \frac{1}{2}(i_L + (-i_{Lk}(t))) = i_L - \frac{1}{2} \frac{V_{C21}}{nL_k}(t-t_0) \quad (27)$$

When the leakage inductor current decreases to zero $i_{Lk}=0$ at t_1 , diodes D_{21} and D_{22} are turned off. From (25), the time interval for mode 1 is

$$T_{10} = t_1 - t_0 = \frac{ni_L L_k}{v_{C21}} \quad (28)$$

Mode 2 (t_1-t_2): at t_1 instant, all the diodes in the transformer secondary side are turned off. L_k and C_r form the resonant circuit. The initial voltage of C_r is $-v_{C21}/n$. The leakage inductor current i_{Lk} and the capacitor voltage v_{Cr} are:

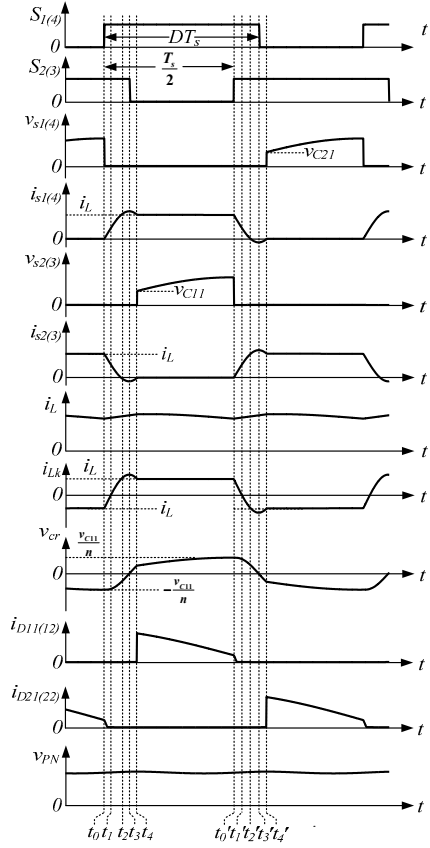


Fig.12 Operation principle of ZCS resonant high step-up full-bridge isolated DC-DC converter with two-cell diode-capacitor network.

$$i_{Lk}(t) = \frac{V_{C21}}{nZ_r} \sin(\omega_r(t-t_1)) \quad (29)$$

$$v_{Cr}(t) = -\frac{V_{C21}}{n} \cos(\omega_r(t-t_1)) \quad (30)$$

Where: $\omega_r = 1/\sqrt{L_k C_r}$ is the resonant frequency. $Z_r(t) = \sqrt{L_k / C_r}$ is the impedance of resonant network.

The current of switch i_{s1} and i_{s4} continue to increase and the current of i_{s2} and i_{s3} continue to decrease.

$$i_{s1}(t) = i_{s4}(t) = \frac{1}{2}(i_L + i_{Lk}(t)) = \frac{1}{2} \left(i_L + \frac{V_{C21}}{nZ_r} \sin(\omega_r(t-t_1)) \right) \quad (31)$$

$$i_{s2}(t) = i_{s3}(t) = \frac{1}{2}(i_L - i_{Lk}(t)) = \frac{1}{2} \left(i_L - \frac{V_{C21}}{nZ_r} \sin(\omega_r(t-t_1)) \right) \quad (32)$$

The leakage inductor current increases and it equals to the boost inductor current $i_{Lk}=i_L$ at t_2 . From (29), the time interval for mode 2 is

$$T_{21} = t_2 - t_1 = \frac{1}{\omega_r} \arcsin\left(\frac{ni_L Z_r}{v_{C21}}\right) \quad (33)$$

Mode 3 (t_2 - t_3): at t_2 instant, the current of switches i_{S2} , i_{S3} decrease to zero and increase reversely. The resonant inductor current i_{Lk} increases to maximum value i_p and the resonant capacitor voltage v_{Cr} decreases to zero. From (31), the maximum value of resonant inductor current i_p and the time interval for mode 3 are

$$i_p = |i_{Lk}(t)|_{\max} = \frac{v_{C21}}{nZ_r} \quad (34)$$

$$T_{32} = t_3 - t_2 = \frac{\pi/2 - \omega_r T_{21}}{\omega_r} \quad (35)$$

Apparently, the condition of ZCS for S_2 and S_3 is: the leakage inductor current peak value should be larger than the boost inductor current $i_p > i_L$.

Mode 4 (t_3 - t_4): at t_3 instant, the resonant inductor current i_{Lk} starts to decrease and the capacitor voltage v_{Cr} continues to increase. Until t_4 instant, i_{Lk} decreases to i_L . The freewheeling diodes of S_2 and S_3 are turned off. The current commutation is completed. Thus, in order to achieve ZCS, S_2 and S_3 should be triggered off between t_2 and t_4 .

Seen from Fig.12, the half of resonant period should be slightly larger than the on-state interval of power switches in one switching time period.

$$\frac{1}{2} T_r \geq (D - 0.5) T_s \quad (36)$$

Where: D is the on-state duty ratio of main switch in the transformer primary side ($0.5 \leq D \leq 1$). $T_s = 1/f_s$ is the switching time period. $T_r = 1/f_r = 2\pi\sqrt{L_k C_r}$ is the time period of resonant circuit.

After t_4 instant, $S_1=S_4=ON$, $S_2=S_3=OFF$, DC source in series with boost inductor charges the resonant capacitor C_r . v_{Cr} increases immediately and diodes D_{11} , D_{12} are conducting. The voltage of resonant capacitor C_r is clamped by C_{11} and C_{12} ($v_{Cr} = n_0/n_1 v_{C11} = n_0/n_1 v_{C12}$). Because the energy stored in L is much higher than that of C_r , this charging interval is very small.

Until t_0' instant, S_2 and S_3 are turned on. The circuit enters into a new time period.

In order to achieve ZCS of main switches, L_k and C_r should be designed to meet $i_p > i_L$ in (34) and (36).

IV. SIMULATION VERIFICATION

Numerical simulations using MATLAB/Simulink have been performed to verify the theoretical analysis and operation principles. The main circuit parameters are: $V_{dc}=48V$, $V_o=540V$, $L_m=400\mu H$, $L_k=8.6\mu H$, $C_r=15\mu F$, $C_{11}=C_{12}=C_{21}=C_{22}=25\mu F$, $L_f=5\mu H$, $C_f=250\mu F$, $T_s=50\mu s$, $n=n_1:n_0=n_2:n_0$, $N=2$.

Fig.13 shows the waveforms of high step-up full bridge isolated DC-DC converter with multi-cell diode-capacitor network ($N=2$) when $V_{dc}=48V$, $V_o=540V$, $n=2$, $R_{Load}=300\Omega$. It

includes the boost inductor current i_L , leakage inductor current i_{Lk} , transformer primary side voltage v_p and the output voltage v_o . In steady state, the duty ratio is $d_{son}=0.65$. The measured voltage gain and voltage stress of power devices are almost consist with the theoretical value.

Fig.14 shows the corresponding waveforms for ZCS resonant high step-up full bridge isolated DC-DC converter. As shown in Fig.14, before main switch is triggered off, the current across MOSFET is smaller than zero. Thus, when MOSFET is turned off, the current is flowing through the freewheeling diode. Then, it is resonant to zero. All the main switches in the transformer primary side achieve ZCS. The unfiltered output voltage v_{pn} just contains some small switching frequency noise. Thus, the volume of output LC filter can be reduced to large extent.

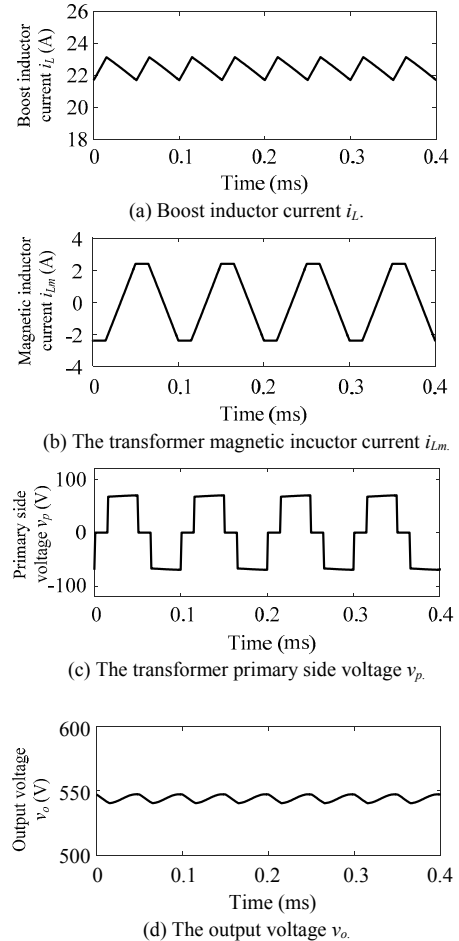
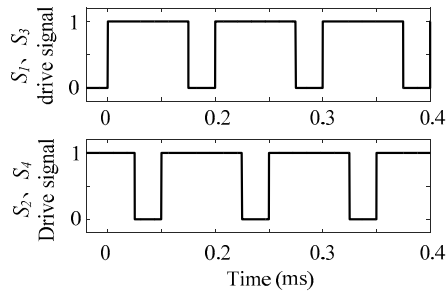
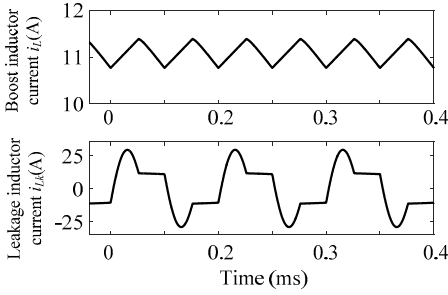


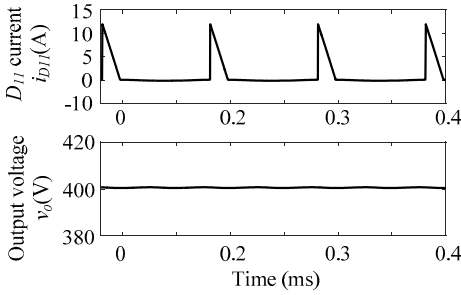
Fig.13 Waveforms of high step-up full-bridge DC-DC converter with multi-cell diode-capacitor network ($d_{son}=0.65$).



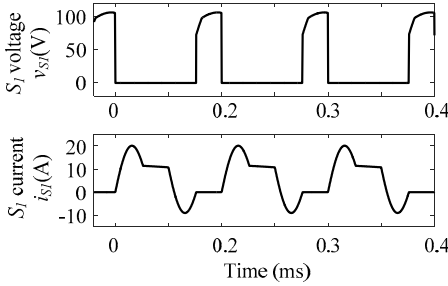
(a) Drive signal.



(b) i_L and i_{Lk} .



(c) Diode current and output voltage.



(d) Switch current voltage and current.

Fig. 14 Waveforms of ZCS resonant high step-up full-bridge isolated DC-DC converter with two-cell diode-capacitor network.

V. CONCLUSION

The full bridge boost DC-DC converter achieves high voltage gain by setting the turns ratio of high-frequency transformer. Conventional boost derived converters with multi-cell diode-capacitor network have inrush current issue and strict LC filter requirement. In order to overcome these drawbacks, this paper proposes a high step-up full-bridge isolated DC-DC converter with multi-cell diode-capacitor network which exploits the features and advantages of multi-

winding transformer and diode-capacitor network. It avoids inrush current issue and achieves almost zero output voltage ripples which reducing the inductance in output LC filter. Meantime, the reduced magnetic component volume contributes to high power density. Furthermore, it can use the leakage inductor of transformer and resonant capacitor to achieve ZCS, which is beneficial to increase efficiency. With improved performance, the new topology is more promising in solar and fuel cell generation system where high step-up voltage boost capability is one of the key requirements.

REFERENCES

- [1] W. Li and X. He, "Review of nonisolated high-step-up dc/dc converters in photovoltaic grid-connected applications", *IEEE Trans. Ind. Electron.*, vol. 58, no. 4, pp. 1239–1250, Apr. 2011.
- [2] Morten Nymand, and Michael A. E. Andersen, "High-efficiency isolated boost DC-DC converter for high-power low-voltage fuel-cell applications", *IEEE Trans. Ind. Electron.*, vol. 57, no. 2, pp. 505–514, Apr. 2010.
- [3] Hassan Benqassmi, Jean-Christophe Crebier, and Jean-Paul Ferrieux, "Comparison between current-driven resonant converters used for single-stage isolated power-factor correction", *IEEE Trans. Ind. Electron.*, vol. 47, no. 3, pp. 518–524, June. 2000.
- [4] Shelas Sathyan, H. M. Suryawanshi, "Soft-switching DC-DC converter for distributed energy sources with high step-up voltage capability", *IEEE Trans. Ind. Electron.*, vol. 62, no. 11, pp. 7039–7050, Apr. 2015.
- [5] Abutbul O, Gherlitz A and Berkovich Y, "Step-up switching-mode converter with high voltage gain using a switched-capacitor circuit," *IEEE Trans. Circuit and System*, vol. 50, no.8, pp. 1098–1102, 2003.
- [6] H. Nomura, K. Fujiwara, and M. Yoshida, "A new dc-dc converter circuit with larger step-up/down ratio," in *Proc. IEEE Power Electron. Spec. Conf.*, 2006, pp. 3006–3012.
- [7] E. H. Ismail, M. A. Al-Saffar, A. J. Sabzali, and A. A. Fardoun, "A family of single-switch PWM converters with high voltage-boosting conversion ratio," *IEEE Trans. Circuits Syst. I, Reg. Papers*, vol. 55, no. 4, pp. 1159–1171, May 2008.
- [8] B. Axelrod, Y. Berkovich, and A. Ioinovici, "Switched-capacitor/switched-inductor structures for getting transformerless hybrid DC-DC PWM converters," *IEEE Trans. Circuits Syst. I, Reg. Papers*, vol. 55, no. 2, pp. 687–696, Mar. 2008.
- [9] Yan Zhang, Jinjun Liu, "Comparison of Conventional DC-DC Converter and a Family of Diode-Assisted DC-DC Converter in Renewable Energy Applications," *Journal of Power Electronics*, vol. 14, no.2, pp. 203-216, March 2014.
- [10] J.-H. Kim, D.-Y. Jung, S.-H. Park, and S.-W. Lee, "High efficiency soft-switching boost converter using a single switch," *Journal of Power Electronics*, vol. 9, pp. 929-939, Nov. 2009.